

Modeling Exposure to Natural Radioactivity in Building Materials

*J.M. Sharaf, M.S. Shekakhwa and T.F. Hussein **

ABSTRACT

Models have been developed to enable prediction of the external gamma dose rate and indoor radon concentration inside a typical dwelling in Jordan.

Concrete and other major construction materials used in Jordan were assessed for ^{40}K , ^{226}Ra and ^{232}Th radioactivity. The external gamma dose rate inside a typical Jordanian room of $4 \times 4 \times 3 \text{ m}^3$ was predicted using the gamma model *GINEX*.

The internal radiation exposure, due to the short-lived decay products of radon that exhales into room air from building materials, was assessed using the radon model. Calculations on concrete were performed to study both diffusive and convective radon transport as well as the effect of pressure gradient on radon exhalation rate. The calculated values were compared with values measured by other authors in some parts of Jordan, and the exposure levels are discussed in terms of limits to the accepted natural levels recommended by the ICRP.

KEYWORDS: Radiation exposure; Radiation dose; Gamma radiation; Radon gas.

INTRODUCTION

During the recent past, increasing attention has been given to the problem of radon exhalation. Direct measurements of indoor exposure have been undertaken in various countries (Battaglia et al., 1984; Hattori et al., 1995) and a review of this subject has been given by Cramer and Burkart (1989). On the other hand, theoretical models and direct code calculations using computer programs to predict the dose that may incur indoors from external gamma radiation and from inhalation of radon progeny, have been recently developed (Brown et al., 1984; Ng et al., 1995). The external radiation exposure is caused by the gamma radiation originating from radionuclides of the uranium and thorium decay chains and from ^{40}K (Shukla, 1995). The internal radiation exposure, mainly affecting the respiratory tract, is due to the short-lived decay products of radon, which exhales into room air from building materials (Samuelsson and Pettersson, 1984). In general, radon progeny concentrations are higher in houses than in the free atmosphere. This is due to additional radon

sources such as tap water, natural gas as well as low rates of air exchange with the free atmosphere (Cramer and Burkart, 1989; Arvela, 1995).

In this study, model calculations were used to predict the external gamma dose-rate and indoor radon concentrations inside an ordinary Jordanian dwelling. Concrete, limestone, ceramic and marble are considered as the main construction materials in different parts of Jordan. These materials were experimentally assessed for ^{226}Ra , ^{232}Th and ^{40}K radioactivity. The measured levels of radioactivity were used to predict the effective dose rate from the two major exposure routes, using two models. The gamma model "GINEX" was constructed to calculate external gamma dose rate inside a typical Jordanian room of $4 \times 4 \times 3 \text{ m}^3$. The radon model takes into account the varying contribution of diffusive and convective radon transport as well as the effect of pressure gradient on radon exhalation rate. Preliminary results obtained with these models are presented and discussed.

External Background Radiation

External background gamma radiation is due to radioactive elements contained inside the rocks that are used in building materials such as: granite, marble,

* Department of Physics, University of Jordan. Received on 18/2/2004 and Accepted for Publication on 16/9/2004.

concrete, fly ash, gypsum, bricks etc. Thorium (^{232}Th), Radium (^{226}Ra), and Potassium (^{40}K) are the most concerned nuclei in the indoor gamma radiation because of their relatively large concentration in building materials.

For a uniformly distributed gamma emitting isotope, the energy flux $\Phi(r, E_i)$ at any point p in air from the isotope in the infinitesimal volume element dV at any other point at a distance r (m) from point p is given by

$$\Phi(r, E_i) = \frac{A(E_i) \cdot E_i \cdot B(r, E_i)}{4\pi} \cdot \frac{\rho_{sample} \cdot e^{-\frac{\mu(E_i) \cdot x}{\rho}}}{r^2} dV \text{ [MeV/m}^2\text{s]} \quad \dots(1)$$

where $A(E_i)$ is the activity concentration of the isotope (Bq/kg), E_i is the gamma-ray energy (MeV), $B(E_i, x)$ is a build up factor, $\mu(E_i)/\rho$ is the mass attenuation coefficient of the medium (m^2/kg), ρ_{sample} is the mass density of the volume element (kg/m^3) and x is the mass thickness of the volume element (kg/m^2).

If the isotope is spread uniformly through the material volume, V , then the effective dose rate, in units of $\mu Sv \cdot h^{-1}$ at point p is computed by the contributions from all the infinitesimal volume elements as

$$\dot{H}_E(r) = \sum_{T_j} w_{T,j} \sum_{E_i} w_{R,i} \cdot f_{rem}(E_i) \times \iiint_V \Phi(r, E_i) \quad \dots(2)$$

where $f_{rem}(E_i)$ is the conversion factor from energy-flux to equivalent-dose rate in units of ($\mu Sv \cdot h^{-1} / (MeV \cdot m^{-2} \cdot s^{-1})$), w_T and w_R are the tissue and the radiation weighting factors, respectively. Taking into account the average occupancy factor and organ shielding factors, the annual effective dose, mSv/y , can be calculated for any organ within an exposed person.

A computer program *GINEX* (*Gamma Indoor EXposure*), was written to perform the direct code integrals in equation (2) for effective-dose rate calculation inside a typical room in Jordanian houses. The program divides the room into rectangular block geometries that include walls, ceiling, and floor and then sums up their contributions to the point of interest. It also allows windows and doors contributions to be subtracted. The *GINEX* inputs include: the gamma ray energies and emissions, tissue or organ weighting factor, radiation weighting factor, energy-flux to effective-dose rate conversion factor, buildup factor, room dimensions, wall thickness and location at which the dose rate is to be

calculated. The program also requires the activity concentration of the ^{226}Ra , ^{232}Th and ^{40}K radionuclides in the construction material as well as the density and mass attenuation coefficient of the materials.

Internal Radon Exhalation

The indoor concentrations of radon and its decay products depend on three factors: the entry or production rate from various sources, ventilation rates, and rates of chemical or physical transformation or removal. Considering only the first two factors, i.e., non-reactive gas, the steady-state activity concentration of radon, C , entering an interior space from effectively internal sources is given by Nazaroff et al. (1988).

$$C = \frac{\sum_i \frac{J_i S_i}{V} + \lambda_v C_o}{\lambda_{Rn} + \lambda_v} \quad \dots(3)$$

where λ_v is the ventilation rate between the room and the outdoor [h^{-1}], C_o is the outdoor activity concentration [Bq/m^3], V is the room volume, J_i is the activity exhalation flux of the source i [$Bq/m^2 \cdot s$], λ_{Rn} is the decay rate of radon [h^{-1}], and S_i is the exhalation area of the source i [m^2].

Exhalation rate from building materials depends on many factors (Janssens et al., 1984). These include Grain-size distribution inside the material, Porosity (ϵ), Moisture content, Permeability (k), Diffusivity, Radium content inside the material, Emanation coefficient, Ventilation and Infiltration.

Transport of radon through building materials can be classified as *flow*, where the fluid (liquid water, air, or water vapor) within the interstitial pore spaces of the material entrains the radon and acts as a carrier, or as *Diffusion* under the influence of a radon concentration gradient between the pore air and external air (Eaton et al., 1984). When radon is transported by either flow or diffusion, the transport takes place in the interstitial pores of the material. The fraction of radon produced and entered the interstitial pores, which is called the emanation coefficient, is therefore a vital parameter in both processes. On the other hand, a pressure gradient or temperature gradient in moisture drives the convective flow of radon content, whereas the diffusion depends on the radon concentration gradient in the material.

The diffusive flux density of radon activity per unit area [$Bq/m^2 \cdot s$]; \vec{J}_{Rn}^d , is expressed by the gradient of radon

concentration in the building material, i.e.,

$$\vec{J}_{Rn}^d = -\varepsilon D_e \vec{\nabla} C_{Rn}. \quad \dots(4)$$

The radon activity flux per unit area due to convective flow; \vec{J}_{Rn}^c , is expressed by

$$\vec{J}_{Rn}^c = C_{Rn} \vec{v}. \quad \dots(5)$$

where v is the superficial velocity vector, which is defined as

$$\vec{v} = -\frac{k}{\mu} \vec{\nabla} P, \quad \dots(6)$$

where k is the intrinsic permeability, μ [kg/ms] is the dynamic viscosity of fluid and P is the pressure.

If the superficial velocity is described by Darcy's law, the material is isotropic and homogeneous with respect to interstitial diffusion coefficient; (D_e), intrinsic permeability; (k), porosity; (ε), emanation coefficient; (f) and radium specific activity concentration; (A_{Ra}), then by assuming incompressible air in the range of pressure of interest, the general transport equation will be given by:

$$\frac{\partial C_{Rn}}{\partial t} = D_e \nabla^2 C_{Rn} + \frac{k}{\mu \varepsilon} \vec{\nabla} P \cdot \vec{\nabla} C_{Rn} - \lambda_{Rn} C_{Rn} + G, \quad \dots(7)$$

where G [Bq/m³s] is the volumetric radon generation rate in the building material pores

$$G = f \rho_s A_{Ra} \lambda_{Rn} \frac{1}{\varepsilon}. \quad \dots(8)$$

where (ρ_s) is the material density.

The total radon activity flux per unit area due to both diffusive transport and convective flow; i.e., exhalation rate; J , in units of [Bq/m²s] is given by

$$\vec{J}_{Rn} = \vec{J}_{Rn}^d + \vec{J}_{Rn}^c = -\varepsilon D_e \vec{\nabla} C_{Rn} + C_{Rn} \vec{v} \quad \dots(9)$$

Indoor Radon Transport Modeling

The main purpose of this model is to find a mathematical solution to the general transport equation including most realistic conditions. By assuming that the superficial velocity consisted in Darcy's law is constant, i.e., the pressure gradient between the wall and the room atmosphere is constant, then, for steady state conditions, the general transport equation is given by

$$\frac{\partial C_{Rn}}{\partial t} = D_e \nabla^2 C_{Rn} - \frac{\vec{v}}{\varepsilon} \cdot \vec{\nabla} C_{Rn} - \lambda_{Rn} C_{Rn} + G = 0, \quad \dots(10)$$

which is an inhomogeneous second order partial differential equation with constant coefficients. The general solution for such an equation includes the solution for the homogeneous equation and a complementary solution for the inhomogeneous term. However, what makes the above equation inhomogeneous is the constant G , and it can be rearranged to become a homogeneous equation as

$$\nabla^2 C_{Rn} - \frac{\vec{v}}{\varepsilon D_e} \cdot \vec{\nabla} C_{Rn} - \frac{\lambda_{Rn}}{D_e} \left[C_{Rn} - \frac{G}{\lambda_{Rn}} \right] = 0. \quad \dots(11)$$

For the case of a room with walls of thickness $2d$, which is much smaller than its other two dimensions, the equation can be reduced to one dimensional equation as:

$$\frac{d^2}{dx^2} C_{Rn} - \frac{v}{\varepsilon D_e} \frac{d}{dx} C_{Rn} - \frac{\lambda_{Rn}}{D_e} \left[C_{Rn} - \frac{G}{\lambda_{Rn}} \right] = 0; \quad \dots(12)$$

The solution of which is found to be

$$C_{Rn}(x) = \frac{G}{\lambda_{Rn}} + e^{lx} \left[A \cosh\left(\frac{x}{\Lambda}\right) + B \sinh\left(\frac{x}{\Lambda}\right) \right], \quad \dots(13)$$

where

$$l^{-1} = \frac{v}{2D_e \varepsilon} \quad \text{and} \quad \Lambda^{-1} = \sqrt{\frac{v^2}{4D_e^2 \varepsilon^2} + \frac{\lambda_{Rn}}{D_e}}.$$

The first boundary condition for the solution is taken from the fact that the concentration inside the wall is maximum, and the derivative $dC_{Rn}(x)/dx$ is zero. Ideal theoretical arguments indicate that this point should be located in the middle of the wall. This is completely theoretical, but for real cases there is a shift from the center of the wall. This shift depends on the pressure and temperature gradients inside the wall as well as the concentration on its both sides. Considering the completely theoretical case

$$\left. \frac{d}{dx} C_{Rn}(x) \right|_{x=0} = 0 \quad \Rightarrow \quad B = -\frac{\Lambda}{l} A.$$

The second boundary condition is taken from the conservation of mass at the steady state condition. For the steady state case and at equilibrium conditions, the exhaled activity concentration into the room should compensate the decrease of the activity concentration inside the room due to decay and ventilation. For a room of depth L , with a radon concentration at the surface of

the wall $C_{Rn}(d)$ the second boundary condition is

$$J_{Rn}(x)|_{x=d} = L\lambda_{Rn}C_{Rn}(x)|_{x=d}, \quad \dots(14)$$

which defines the constant A as:

$$A = \frac{G}{\lambda_{Rn}} \frac{e^{-d/l}}{[Cosh(\beta) - \gamma Sinh(\beta)] + \alpha\beta[Sinh(\beta) - \gamma Cosh(\beta)]} \quad \dots(15)$$

where

$$\beta = \frac{d}{\Lambda}, \quad \gamma = \frac{\Lambda}{l}, \quad \text{and} \quad \alpha = \frac{\varepsilon D_e}{d} \frac{1}{\left[L\lambda_{Rn} - \frac{v}{2} \right]},$$

and equation (13) can be written now in the form

$$C_{Rn}(x) = \frac{G}{\lambda_{Rn}} + Ae^{\frac{x}{l}} \left[Cosh\left(\frac{x}{\Lambda}\right) - \gamma Sinh\left(\frac{x}{\Lambda}\right) \right], \quad \dots(16)$$

while the exhalation rate flux is given by

$$J_{Rn}(d) = v \frac{G}{\lambda_{Rn}} \left(1 - \frac{1/2}{\left(1 + \alpha\beta \frac{Sinh(\beta) - \gamma Cosh(\beta)}{Cosh(\beta) - \gamma Sinh(\beta)} \right)} \right) + \frac{G}{\lambda_{Rn}} \frac{\varepsilon D_e}{\Lambda} \left(\frac{1}{\left(\alpha\beta + \frac{Cosh(\beta) - \gamma Sinh(\beta)}{Sinh(\beta) - \gamma Cosh(\beta)} \right)} \right) \quad \dots(17)$$

Note that equations (16) and (17) are solutions for the general transport equation that includes *diffusive* and *convective* radon transports inside the walls. Nevertheless, solution to the diffusive transport equation; equation (16), is obtained by ignoring the convective transport in equation (10); i.e. $v=0$. This implies that

$$l^{-1} = 0, \quad \Lambda^{-1} = \sqrt{\frac{\lambda_{Rn}}{D_e}}, \quad \beta = \frac{d}{\Lambda}, \quad \gamma = 0, \quad \text{and} \quad \alpha = \frac{\varepsilon D_e}{dL\lambda_{Rn}},$$

and then the solutions are given by

$$A = \frac{-G/\lambda_{Rn}}{Cosh(\beta) + \alpha\beta Sinh(\beta)},$$

$$C_{Rn}(x) = \frac{G}{\lambda_{Rn}} + A Cosh(\beta),$$

and

$$J_{Rn}(d) = \varepsilon G \sqrt{\frac{D}{\lambda_{Rn}}} \frac{Sinh(\beta)}{Cosh(\beta) + \alpha\beta Sinh(\beta)}$$

Results and Discussion

1) Measurement of Radioactivity Concentrations

Samples of locally available building materials were randomly selected from different parts of Jordan. Each sample (0.275 kg) was powdered, sealed in cylindrical plastic container (5 cm diameter and 5 cm height) and stored for four weeks before counting. Measurement of the activity concentration of the samples was carried out by the use of standard high-resolution gamma spectrometry. The low level gamma spectrometer consisted of an HPGe detector (1.72 keV resolution at 1.33 MeV), which was suitably connected to an Accuspec PC-based MCA for spectroscopic analysis. The counting time for each sample was 60,000 s. The activity concentrations of ^{226}Ra , ^{232}Th and ^{40}K were determined by calibrating against reference materials (IAEA, 1987), RGU-1, RGTh-1 and RGK-1, respectively. The analysis procedure is similar to that described by Savidou et al. (1995). Table 1 lists measured specific activities for various building materials used in Jordan.

2) External Background Radiation Modeling

Houses with concrete walls usually have concrete floors covered with tiles and the ceilings are always concrete. Hence; as a preliminary evaluation of *GINEX* program, concrete with density of $2.35 \times 10^3 \text{ kg/m}^3$ was taken as the only building material used in the construction of the model room. The room was assumed to have dimensions of $4 \times 4 \times 3 \text{ m}^3$ with wall thickness of 0.1 m , which is typical for the Jordanian houses. The room also has two, $1.5 \times 2 \text{ m}^2$, windows each centered on a wall, and a $1.5 \times 2 \text{ m}^2$ door centered on a third wall (see Fig. 1). The dose rate was calculated at the center of the room one meter above the floor level. The atmosphere inside the room is assumed to be dry-air with density of 1.169 kg/m^3 , at STP (Weast, 1980). Mass attenuation coefficients, buildup factor, and energy-flux to effective dose rate conversion factor were taken from literature values (Takeuchi et al., 1986 and Hubbell, 1982). With these conditions, the effective-dose rate predicted by *GINEX* program, after 100 iterations, was 0.494 mSv/y , which is higher than the annual average effective dose of 0.45 mSv , reported by UNSCEAR (1993).

Further, the gamma dose rate in air, at 1 m above the floor level, was measured using a portable ionization chamber (*Babyline, 91*), inside 10 different rooms with dimensions similar to that of the model room. The average

value of the dose rate, obtained after subtraction of the cosmic ray contribution (20 nGy.h^{-1}) was found to be 118 nGy.h^{-1} , which corresponds to an effective dose rate of 0.577 mSv/y using a conversion factor of 0.7 Sv/Gy and an occupancy factor of 0.8 . This is higher than the predicted value by about 14% , which is expected since contributions of many other sources, i.e. soil beneath the flooring, terrestrial radiation and ambient radon due to air exchange, were not taken into consideration in the calculated result. For example, the absorbed dose rate resulting from the terrestrial radioactivity of soil beneath the model room flooring is estimated to be 7.0 nGy.h^{-1} from the known levels of radionuclides and the attenuation due to the flooring. This is equivalent to an effective dose rate of 0.034 mSv/y and if that is added to the value predicted by *GINEX*, the final dose rate comes to 0.528 mSv/y , or 8% lower than the measured value. Also, the difference is expected to be much lower if the dose rate due ambient radon is taken in consideration. Nevertheless, the *GINEX* program could be of use to provide an estimate of average indoor dose rate from the concentration of radionuclides present in different building materials and this should be of great help in deciding on upper bound limits of natural radioactivity content in such materials.

3) Indoor Radon Transport Modeling

In the development of the radon model, some different runs have been performed in order to calibrate the model against measured data. Predicted values were compared with values measured by another group in an area north of Jordan, Ramtha and its territories (Abdeljawad, 1994). Model predictions which do not take convective transport into account are, nevertheless, less than the measured values and therefore, it was decided to include this factor in an attempt to match the model predictions with measured values. The critical term here is the Darcy's velocity,

$$\vec{v} = -\frac{k}{\mu} \vec{\nabla}P,$$

which includes the permeability; k , fluid viscosity; μ , and the pressure gradient, $\vec{\nabla}P$. Permeability can be estimated as an order of magnitude by the definition given by Nazaroff et al. (1988).

$$k = \frac{c\varepsilon^2}{TS^2}.$$

where c is a constant that depends on the pore shape

and varies between 0.5 and 0.67 , T is an empirical factor called tortuous factor which accounts for the fact that the flow channels are not straight, with a value greater than or equal to 1.0 . S is the specific surface area that is given by $S=6(1 - \varepsilon)/D$ for uniform spherical particles, where D is the particle diameter. Hence, k is in the order of $10^{-39} [\text{m}^2]$. Fluid viscosity for dry air at standard conditions is $1.81 \times 10^{-5} [\text{kg/m.s}]$. Therefore, Darcy's velocity was taken in the order of $10^{-31} [\text{m/s}]$, where the pressure gradient is considered to be $10^4 [\text{kg/m}^4]$, that corresponds to 10 Pascal pressure difference and 0.05 m wall half-thickness. Other parameters required for the model evaluation are listed in Table (2).

The average outdoor radon concentration using 55 measurements distributed in different sites of Ramtha and its territories was 0.32 Bq/m^3 . While the average indoor radon concentration was 3.84 pCi/L or 142.10 Bq/m^3 as reported by Abdeljawad (1994).

In order to test the model under different ventilation conditions, the indoor radon concentration was calculated for three ventilation rates. These rates are called high, moderate, and low that correspond to $\lambda_v \lambda$ values, greater than 1 , between 1 and 0.3 , and lower than 0.3 h^{-1} , respectively (Ng *et al.*, 1995). The indoor radon concentration was also estimated for different drift velocity values. Results obtained are presented in Table (3).

It can be seen from the data shown in Table (3) that the estimated indoor radon concentration ranged from about 17 to 182 Bq/m^3 due to both seasonal variation and pressure gradient. The concentration tends to be higher in winter (low ventilation rate) and decreases gradually towards the hot seasons as the ventilation rate improves. It also increases with increasing Darcy's velocity or the pressure difference between the walls and the room atmosphere which in turn is a function of temperature. Saturation value for indoor radon concentration is obtained for Darcy's velocity value of 10^{-13} m/s , while its actual value is in the order of 10^{-30} m/s . Nevertheless, indoor radon concentration generated by this model is greater than that generated by the diffusive transport model even if the Darcy's velocity is very small. However, both models will match to each other when $v=0$. It should be noted also that the measured values are within the predicted radon concentration range if ventilation conditions are taken into account.

In the last few years, sophisticated dosimetric models have been developed to evaluate doses to the sensitive

tissue in the lung resulting from the inhalation of radon and radon decay products (Harley, 1988; Robbins and Meyers, 1995). The dose to the respiratory tract depends on the radon concentration in air, radon daughter equilibrium factor, breathing rate and fraction of time spent indoors. All these parameters are highly variable and therefore a number of assumptions are required to calculate the “whole-body dose equivalent” from exposures of the respiratory tract. For our considerations, a conversion factor of 0.061 *mSv/y* per *Bq/m³* for 80% time spent indoors (UNSCEAR, 1982), was adopted. Using a mean value of 34.86 *Bq/m³* for indoor radon concentration and an equilibrium factor of 0.5 for radon daughters, the effective dose equivalent will be in the range of 1 *mSv/year*. A comparison with what is normally accepted for the general public from the exposure to ionizing radiation from other sources, i.e 1 *mSv/y*, shows the extent of the radon problem.

CONCLUSIONS

Two computer models were used to compute the external gamma dose rate and indoor radon concentration in a typical Jordanian room. *GINEX* model provides an estimate of the annual effective dose rate inside a typical room using measured radioactivities in building materials. The value obtained after 100 iterations was 0.494 *mSv*, which is 14% lower than the measured value of 0.577 *mSv*. The rather low value predicted for the annual effective dose rate probably reflects the need for

the model to take into account the possible contribution of the outdoor or the environmental dose rate to the indoor dose rate. Nevertheless, both calculated and measured values are close to that of the worldwide average of 0.45 *mSv* (UNSCEAR, 1993).

Radon transport model was used to estimate the indoor radon concentration, due to the short-lived daughter products of radon that exhales into room air from building materials. The model deals with diffusive and convective radon transport. Predicted values were comparable with those measured previously by other researchers. Discrepancy between the single room model and occurrence of radon in real dwellings as well as the omission from the model the possible contribution of the soil gas radon to the radon concentration, are the factors most affecting the difference between measured and predicted results. In addition, the model showed the dependency of radon transport on pressure gradient even if Darcy’s velocity is very small and proved that the differences in ventilation practices is one of the factors strongly affecting radon concentration inside dwellings.

Finally, both models suggest that the building materials are the main sources of external gamma dose and indoor radon concentration in Jordan. The use of concrete structures is very common in Jordan and this, however, increases the dose rates and the indoor/outdoor ratio compared to other countries where houses have either some of the walls or ceiling built of wood in order to avoid building materials with strong radon exhalation.

Table 1: Measured values of specific activity concentrations for various building materials used in Jordan.

Building Material	Specific Activity Concentration [Bq/kg]		
	⁴⁰ K	²²⁶ Ra	²³² Th
Sand	197±38	08±11	10±01
Gravel	152±17	10±08	12±03
Lime-stone	163±32	10±09	4±01
Marble	132±11	12±09	4±01
Cement	185±19	20±09	12±05
Ceramic	543±41	29±11	40±09
Concrete	369±40	41±07	34±07

**Table 2: Required parameters to evaluate the radon transport model
(Brown *et al.*, 1984 and Nero *et al.*, 1984).**

<i>Parameter</i>	<i>Symbol</i>	<i>Value</i>
<i>Interstitial diffusion coefficient</i>	D_e	$3.3 \times 10^{-8} \text{ m}^2/\text{s}$
<i>Porosity</i>	ε	0.068
<i>Emanation coefficient</i>	f	0.25
<i>Radon decay constant</i>	λ_{Rn}	$2.1 \times 10^{-6} \text{ s}^{-1}$
<i>Half thickness of the wall</i>	d	0.05 m
<i>Density of the material</i>	ρ_s	2300 kg/m ³

**Table 3: Calculated indoor radon concentration (Bq/m^3)
for different Darcy's velocities and different ventilation rates inside an ordinary Jordanian room.**

<i>Darcy's velocity</i> [m/s^2]	<i>Indoor radon concentration (Bq/m^3)</i>		
	<i>Low</i>	<i>Moderate</i>	<i>High</i>
10^{-13}	57.08	34.86	17.78
10^{-12}	57.08	34.86	17.78
10^{-11}	57.09	34.87	17.78
10^{-10}	57.14	34.90	17.80
10^{-9}	57.68	35.23	17.96
10^{-8}	63.43	38.72	19.73
10^{-7}	182.64	111.27	56.39

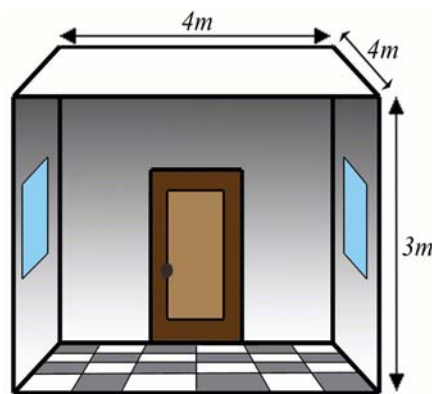


Figure 1: Sketch of the model room used in GINEX program.

REFERENCES

- Abdeljawad, Z. 1994. Radon Gas Concentration Measurement in Dwellings Air and Outdoor Air in Ramtha Territory-Jordan, Master Thesis, Yarmouk University, Irbid, Amman. (Arabic Thesis).
- Arvela, H. 1995. Seasonal Variation in Radon Concentration of 3000 Dwellings with Model Comparisons. *Radiation Protection Dosimetry*, 59(1): 33-42.
- Battaglia, A. Bazzano, E. and Carioni, T. 1984. Indoor Dose in Milan. *Radiation Protection Dosimetry*, 7(1-4): 283-285.
- Brown, K. Dimbylow, P. J. and Wilkinson, P. 1984. Modeling Indoor Exposure to Natural Radiation. *Radiation Protection Dosimetry*, 7(1-4): 91-94.
- Cramer R. and Burkart W. 1989. The Radon Problem. *Radiat. Phys. Chem.*, 39(2):251-259.
- Eaton, R.S. and Scott, A.G. 1984. Understanding Radon Transport into Houses. *Radiation Protection Dosimetry*, 7(1-4): 251-253.
- Harley, N. 1988. Interaction of Alpha Particles with Bronchial Cells. *Health Physics*, 55: 665-669.
- Hattori, T. Ichiji, T. and Ishida, K. 1995. Behavior of Radon and its Progeny in a Japanese Office. *Radiation Protection Dosimetry*, 62(3): 151-155.
- Hubbell, J.H. 1982. Photon Mass Attenuation and Energy-Absorption Coefficient from 1keV to 20MeV. *J. Appl. Radiat. Isot.*, 33: 1269-1290.
- IAEA. 1987. Preparation and Certification of IAEA Gamma-ray Spectrometry Reference Materials RGU-1, RGTH-1 and RGK-1, *Report IAEA/RL/148*, Vienna.
- Janssens, A. Raes, F. and Poffijn, A. 1984. Transients in the Exhalation of Radon Caused by Changes in Ventilation and Atmospheric Pressure. *Radiation Protection Dosimetry*, 7(1-4): 81-86.
- Nazaroff, W. W. and Nero, A. V. 1988. *Radon and its Decay Products in Indoor Air*. John Wiley and Sons, USA.
- Nero, A. V. and Nazaroff, W. W. 1984. Characterising the Source of Radon Indoors. *Radiation Protection Dosimetry*, 7(1-4): 23-39.
- Ng, C.Y., Leung, J.K.C. and Tso, M.Y.W. 1995. Modeling Exposure to Naturally Occurring Radionuclides in Building Materials. *Radiation Protection Dosimetry*, 59(1): 43-48.
- Robbins, E. and Meyers, O. 1995. Cycling Cells of Human and Dog Tracheobronchial Mucosa: Normal and Repairing Epithelia. *Technology: J. of the Franklin Inst.*, 332A: 35-42.
- Samuelsson, C. and Pettersson, H. 1984. Exhalation of ²²²Rn from Porous Materials. *Radiation Protection Dosimetry*, 7(1-4): 95-100.
- Savidou, A. Raptis, C. and Kritidis, P. 1995 Natural Radioactivity and Radon Exhalation from Building Materials used in Attica Region, Greece. *Radiation Protection Dosimetry*, 59(4): 309-312.
- Shukla, V., Sadasivan, S., Sundaram, V. and Nambi, K. 1995. Assessment of Gamma Radiation Exposure Inside A Newly Constructed Building and A Proposed Regulatory Guideline for Exposure Control from Natural Radioactivity in Future Buildings. *Radiation Protection Dosimetry*, 59(2): 127-133.
- Takeuchi, K. and Tanaka, S. 1986. Absorbed-Dose and Dose-Equivalent Buildup Factors of Gamma Rays Including Bremsstrahlung and Annihilation Radiation for Water, Concrete, Iron, and Lead. *Appl. Radiat. Isot.*, 37(4): 283-296.
- UNSCEAR. 1982. Ionising Radiation: Sources and Biological Effects. Report to the General Assembly, with Annexes, United Nations, New York
- UNSCEAR. 1993. Sources and Effects of Ionizing Radiation. UNSCEAR 1993 Report. United Nations, New York.
- Weast, R.C. and Astle, M.J. 1980. *Handbook of chemistry and Physics*, 60th Edition. CRC Press, USA.

*

	(^{232}Th)	(^{226}Ra)	(^{40}K)
(GINEX)	(4X4X3 m ³)	" "	" "
			:

.2004/9/16

2004/2/18

*